

# Tunable semiconductor lasers for telecommunications applications

H. Debrégeas-Sillard, A. Plais, A. Vuong, Th. Fillion, D. Locatelli, J. Decobert, D. Herrati,  
P. Doussi re\*, J. Jacquet

*Alcatel CIT – OPTO+, Route de Nozay, 91460 Marcoussis, France*

*\*Alcatel Optronics, Route de Villejust, 91625 Nozay, France*

*[helene.sillard@alcatel.fr](mailto:helene.sillard@alcatel.fr)*

We present the various currently studied tunable lasers designs, then focus on recent optimizations and performances on 3-section DBR lasers (16nm tuning, 20mW coupled output power), electronic control, aging, and new functionalities integration (amplifier, modulator).

**Keywords:** tunable lasers, distributed Bragg reflector, wavelength agility, integrated semiconductor amplifier, integrated modulator

## Introduction

Tunable lasers are becoming important elements in optical networks to reduce costs. They could be used particularly for systems monitoring : a reference signal is transmitted and detected on each wavelength, thus informing on transmission quality. Or inventory costs could be drastically reduced by using tunable lasers as sparing sources or even as standard sources, to avoid the obligation of owning 2 or 3 sets of fixed wavelength sources covering the whole transmission band.

Besides, with the increasing bit rate at the user level (data traffic, Fiber To The Home (FTTH)), flexibility and wavelength agility are becoming critical for routing in optical networks. Would it be to add a new wavelength in an Add and Drop, as emission lasers in 3R electro-optic regenerators, or as tunable clocks in 3R all-optical regenerators,... In such applications, tuning speed is a key characteristic : it should be a few milliseconds for circuit switching, and down to a few nanoseconds for packet switching.

Currently used sources are Distributed Feedback Lasers (DFB). To take their place, tunable lasers must not only provide maximum tunability, but also similar characteristics (20mW coupled output power, spectral linewidth below 10MHz, ...), long-term reliability, and efficient control electronics, while maintaining limited overcost (below 20%).

In most applications, signal is 10Gb/s modulated, with excellent characteristics (extinction ratio over 10dB, low chirp, square eye diagram). Thus the integration of a modulator section is a promising research way.

## 1. Different types of tunable or selectable lasers

To face the growing demand for tunable lasers, many laboratories proposed different solutions, aiming at the various applications. Three types of tunable lasers emerged :

- **Thermally tuned distributed feedback (DFB) lasers**

The wavelength emitted by a DFB lasers varies with temperature by about  $0.9 \text{ \AA}/^\circ\text{C}$ , leading to 4nm tuning for  $45^\circ\text{C}$  temperature range.

To increase the achievable tuning range, cascaded DFB lasers are proposed [1] : the device is made of three DFB lasers, with different grating pitches corresponding to 5nm spaced Bragg wavelengths. Each DFB section is thermally tuned to cover 5nm tuning, leading to 15nm total tuning range, with temperature ranging between  $-5$  and  $+50^\circ\text{C}$ .

Another solution consists in fabricating a DFB array (up to 12 DFB lasers), with Bragg wavelength spacing around 2.5nm. The DFB waveguides are then combined by a multimode interferometer (MMI) [2], or more recently by a micro electro-mechanical (MEMs) mirror [3]. One

wavelength is selected by turning on the corresponding DFB laser, and off the others. Temperature enables fine wavelength control. 20mW fiber coupled power over 33nm (C-band) have been obtained [3].

These devices have the advantage of using very well-known and reliable DFB lasers, and wavelength control is extremely simple. But with such large temperature ranges, these solutions are very power consuming. And due to extremely long time constants of thermal effects, they can only provide slow tuning (no routing applications).

- **Mechanically tuned lasers**

To reduce tuning speed and further increase tuning range, while maintaining easy-to-control continuous tuning, solutions with mechanical modifications of the laser cavity geometry are proposed.

Firstly, external cavity lasers, where the gain medium is a high power semiconductor laser diode. The emerging beam is collimated, and diffracted on an external grating. The emitted wavelength is imposed by the incidence angle on the grating, and the Fabry-Perot modes position. Continuous tuning is obtained by synchronously varying the grating angle and the cavity length. For example 40nm tuning, with 10mW output power, with less than 15ms switching time have been obtained [4].

Secondly, vertical cavity surface emitting lasers (VCSELs), where one Bragg mirror is a MEMs. Due to the very small cavity length, only one Fabry Perot mode lases in the gain spectrum. This mode is continuously tuned by translating the MEMs mirror. With 1310nm optical pumping, 20mW over the whole C-band have been obtained [5].

- **Current injection tuned lasers**

The refractive index of a quaternary material, at a wavelength above its photoluminescence wavelength, decreases when injecting carriers, due mainly to plasma effect. Many tunable lasers are based on this phenomenon : a passive section (called Bragg section), with a Bragg grating, imposes the emission wavelength, which is modified by current injection. Gain is provided by an active section, made of active material multi quantum wells (MQW). Fine tuning is obtained by modifying the index of a phase section with current injection as well. These devices provide fast tuning, large output power, and the simplicity of integrated components. But they require sophisticated electronic control algorithms to ensure mode hop free behavior.

The basic device is a distributed Bragg reflector (DBR) laser. It will be presented in detail in this paper. The Bragg section contains a standard Bragg grating. Tuning range is limited by the achievable Bragg section refractive index :  $\Delta\lambda/\lambda = \Delta n_{\text{Bragg}} / n_{\text{Bragg}}$  : 16nm tuning, with 20mW coupled output power have been demonstrated [6,7].

Other structures have been proposed, based on tuning mechanisms where  $\Delta\lambda/\lambda$  is no longer limited to  $\Delta n_{\text{Bragg}} / n_{\text{Bragg}}$ . The first structure is the grating coupler sampled reflector laser (GCSR). It relies on a tunable intracavity grating-assisted codirectional coupler filter, that tunes as  $\Delta n_{\text{passive}} / (n_{\text{g passive}} - n_{\text{g active}})$ , where  $n_{\text{g passive}}$  and  $n_{\text{g active}}$  are the group mode indexes of the passive and active piled up waveguides respectively : 40nm tuning with more than 3mW have been demonstrated [8].

The other structure consists of a gain and phase shifter section between two sampled grating distributed reflectors (SG-DBR). A sampled grating is a conventional grating with grating elements removed in a periodic fashion, leading to reflection spectra with periodic maxima. Same types of reflection spectra can be obtained as well with superstructure gratings : grating pitches is linearly with a large periodicity (SSG-DBR). The periods of the two spectra are slightly mismatched : lasing occurs at that pair of maxima that are aligned. Phase shifter is adjusted to place a mode at this

wavelength as well. Inducing small index changes in one mirror relative to the other causes adjacent reflectivity maxima to come into alignment, shifting the lasing wavelength a large amount for a small index change : this is the “Vernier effect”. The total tuning range is only imposed by the active section gain bandwidth, and by the tradeoff with side mode suppression ratio (SMSR). 40nm tuning can thus be achieved, with 4mW coupled output power [9]. Power is limited because light is transmitted through a grating, and not directly from the gain section. To overcome this, a semiconductor optical amplifier (SOA) front section is added, leading to 20mW coupled output power [10]. These devices provide excellent performances, but at the expense of a large number of sections (5), and extremely complicated control electronics. A more precise comparison is given at the end of the paper (§6).

Recently, a new device has been proposed, with a sampled grating rear section, and multiple Bragg gratings with independent current controls for the front section. Tuning current applied to one or two of the front gratings selects a wavelength band across which one line from the rear phase grating reflector is scanned to provide continuous tuning. 45nm tuning with 28mW facet output power have been demonstrated [11].

## 2. 3-section DBR laser

Among all these solutions, 3-section DBR laser appears as a good compromise between simplicity (only three control currents, standard technological process), tuning range (16nm tuning), power (20mW coupled without any additional semiconductor amplifier section), and fast switching (<1ms). This section presents the basic behavior of a DBR laser, then the different optimizations, and at last static and dynamic results.

### 2.1 DBR laser principle

The device is illustrated in figure 1.

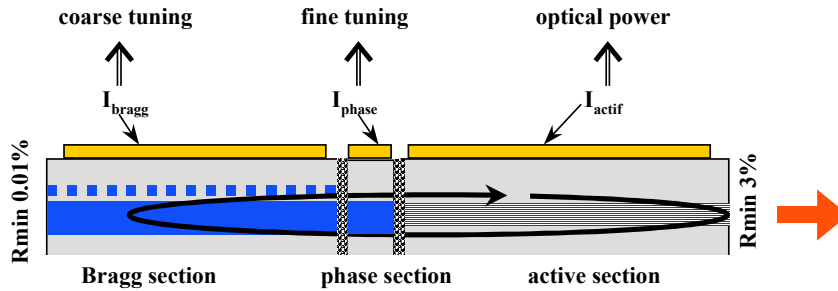


*figure 1 : 3-section DBR laser scheme*

Optical power is provided by injecting current ( $I_{active}$ ) in the multiple quantum wells (MQW) of the active section.

The maximum reflection wavelength of a Bragg grating is given by  $\lambda = 2 \cdot n_{eff} \cdot \Lambda$ , where  $n_{eff}$  is the effective index, and  $\Lambda$  the grating pitch. In a DFB laser, grating is etched in the active section. Above threshold, carriers density is blocked, so the emission wavelength is almost constant.

On the contrary, in a DBR laser, the emission wavelength is imposed by a grating etched in another section, in passive quaternary material, called Bragg section. The carrier density  $N$  in this section is not blocked, and increases when injecting current, through relation

$$I_{Bragg} = I_{leakage} + eV (AN + BN^2 + CN^3) \quad (1)$$

where  $I_{Bragg}$  is the injected current,  $I_{leakage}$  is the sum of leakage currents,  $e$  is the electron charge,  $V$  the undoped volume, and  $A$ ,  $B$  and  $C$  are parameters specific to the material. Through free-carrier absorption and bandfilling, the Bragg section effective index varies as :

$$\Delta n_{eff} = \Gamma \cdot \frac{dn_Q}{dN} \cdot \Delta N \quad (2)$$

where  $\Gamma$  is optical confinement in quaternary material,  $dn_Q / dN$  is the quaternary index variations with carrier density (negative value), and  $\Delta N$  is the carrier density variation due to  $I_{Bragg}$ . This leads to a decrease of the Bragg section maximum reflection wavelength  $\lambda_{Bragg}$ :

$$\Delta \lambda_{Bragg} = 2 \cdot \Delta n_{eff} \cdot \Lambda \quad (3)$$

As shown in figure 1, light is partially reflected by the active section facet. And for wavelengths close to  $\lambda_{Bragg}$ , light is reflected by the Bragg grating, with a penetration length noted  $L_{eff}$ . Thus, we obtain a Fabry-Perot cavity, with optical length  $n_{gactive} \cdot L_{active} + n_{gphase} \cdot L_{phase} + n_{gBragg} \cdot L_{eff}$ . Laser emits on the Fabry-Perot mode closest to  $\lambda_{Bragg}$ . When injecting current in the phase section ( $I_{phase}$ ), the Fabry-Perot cavity modes are shifted, due to  $n_{gphase}$  variations (figure 2).

The SMSR is maximal when the Fabry-Perot mode wavelength coincides with the maximum Bragg reflectivity wavelength ( $\lambda_{FP} = \lambda_{Bragg}$ ), and a mode hop occurs (with SMSR minimum) when two Fabry-Perot modes are equidistant from Bragg wavelength. Typical emission wavelength and SMSR characteristics as a function of  $I_{Bragg}$  are represented in figure 3. The wavelength levels correspond to Fabry-Perot modes, successively selected by the Bragg reflectivity spectrum, when injecting  $I_{Bragg}$ . Tuning efficiency is maximum for low Bragg currents, due to the 3<sup>d</sup> degree polynomial variation of equation (1). For higher Bragg currents, thermal effects tend to compensate for injection-induced tuning, eventually increasing emission wavelength. The low SMSR values at first mode hops are caused by Bragg section current source noise. The effect is less frequent for large Bragg current, due to lower tuning efficiency.

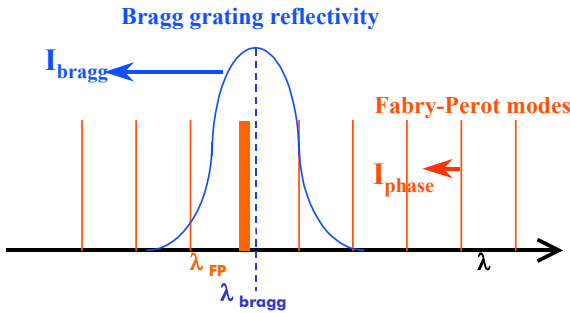


figure 2 : DBR tuning mechanism

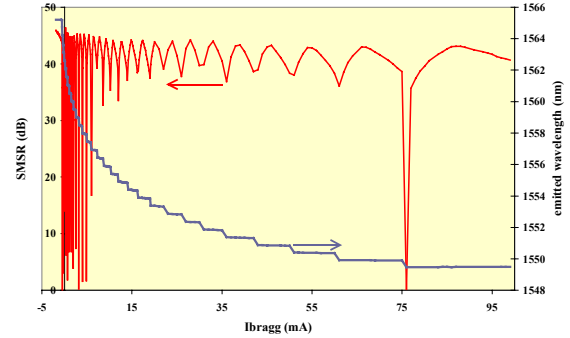


figure 3 : typical wavelength and SMSR variations with  $I_{Bragg}$

## 2.2 DBR design optimizations

### • Vertical structures optimization

According to equation (2), tuning range is proportional to optical confinement in quaternary material, and its index variations with injected current. Thus a very thick quaternary, with photoluminescence wavelength close to emission wavelength is preferred.

But for large power emission, the optical mode must be deconfined in the active section (to reduce losses and improve fiber coupling efficiency), overlap between active and passive sections modes must be maximized, and passive material photoluminescence wavelength should be far from emission wavelength to reduce absorption.

The adopted structures are thus a compromise between all these requirements :

- Active section is made of six 8nm thick Q1.5 compressively strained quantum wells, and five 10nm thick Q1.18 barriers, surrounded by 50nm thick undoped Q1.18 confinement layers.

- Bragg section is made of 380nm thick Q1.42 bulk material, and 70nm Q1.18 grating layer, separated by 100nm InP spacer.
- Phase section is similar to the Bragg section, except for the grating that is etched during process.

A 1.5 $\mu\text{m}$  wide ridge waveguide is then etched, and buried in p-doped InP. Sections are isolated by electrode and InGaAs heavily doped contact layers etching, plus deep ion implantation to suppress any interelectrodes leakage current.

- Sections lengths

Active section length has been optimized at 600 $\mu\text{m}$ , as it provides high output power, low threshold current, and good external efficiency, while maintaining reduced serial resistance, limiting thermally induced power saturation.

Phase section length is chosen about 50 $\mu\text{m}$ , that are sufficient to shift Fabry-Perot modes comb by the free spectral range (FSR) for limited injected current.

Bragg section length must be sufficient to have a high reflectivity and obtain single-mode behavior. But we observed that when increasing length, tuning range decreases due to injected carriers consumption for spontaneous amplified emission (2nm tuning range decrease for Bragg length 500 $\mu\text{m}$  instead of 300 $\mu\text{m}$  [7]).

- Grating coupling efficiency  $\kappa$

The Bragg grating coupling efficiency  $\kappa$  has a strong impact on DBR operation. With a strong  $\kappa$ , Bragg section reflectivity spectrum is wide : the grating is weakly wavelength selective, with strong reflectivity.  $L_{\text{eff}}$  is thus small, enabling small Bragg lengths. But the least Fabry-Perot comb irregularity may provoke lasing on a side mode, leading to tuning curves irregularities. The device is thus extremely sensitive to any parasitic cavity (due to butt joint, Bragg facet).

On the other hand, a weak  $\kappa$  value releases from parasitic cavities, and generates stronger SMSR and power variations among each mode, which makes device control easier as shown further in §3. But  $L_{\text{eff}}$  is longer, imposing a long Bragg section, thereby reducing tuning range. The spectral linewidth is degraded too, due to Bragg current source noise, that creates Bragg index variations, and consequently wavelength scattering.

$\kappa$  around 40cm<sup>-1</sup> has been chosen as a standard value, leading to 300 $\mu\text{m}$  Bragg section length.

- Active section ridge design

To improve coupled output power, beam divergence from active section has been reduced with a lateral taper represented in figure 4. With a ridge width varying from 1.5 $\mu\text{m}$  to 0.8 $\mu\text{m}$  along the last 200 $\mu\text{m}$  of the active section, beam divergence has been reduced to 16° x 20° (compared to 20° x 25° for a 1.5 $\mu\text{m}$  straight ridge), and 75% coupling efficiency is now typical (compared to 60%).

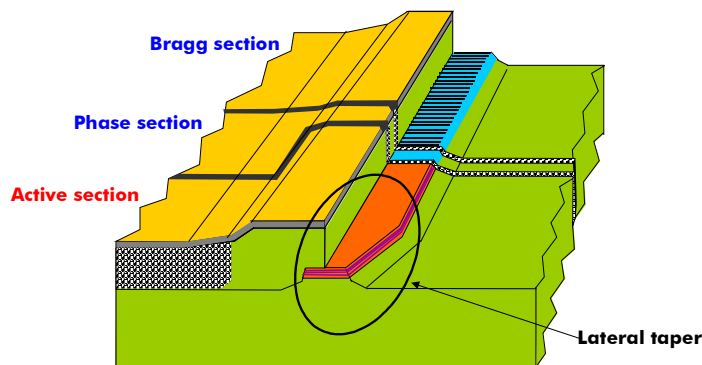


*Figure 4 : schematic view of the DBR laser, with tapered active section.*

### 2.3 Static results

With this optimized structure, we reproducibly obtain tuning over around 16nm, with SMSR above 40dB apart from mode hops (figure 3). As output power decreases with  $I_{\text{Bragg}}$ , due to free-carrier absorption in the Bragg section, the achievable output power is imposed by the least favorable operating conditions, that is maximum  $I_{\text{Bragg}}$ . As shown in figure 5, 20mW can be fiber coupled for all the modes at  $I_{\text{active}} < 200\text{mA}$ , with 14.2dBm maximum power at  $I_{\text{active}}=320\text{mA}$ . Half of the C-band is thus covered (40 channels 50GHz-spaced), with 20mW coupled (figure 6).

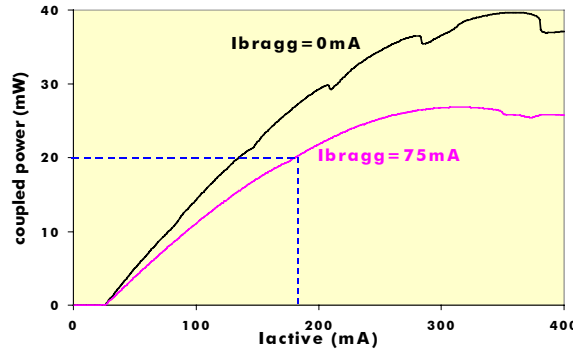


*figure 5 : fibre coupled power versus  $I_{\text{active}}$ , for extreme  $I_{\text{Bragg}}$  values.*

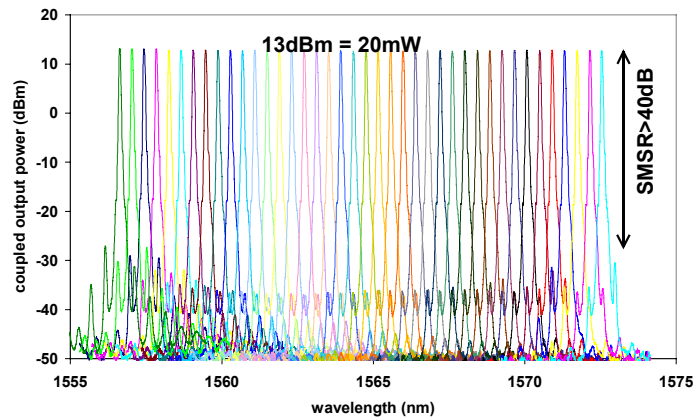


*figure 6 : superimposed addressable spectra : 16nm, with 20mW fiber coupled power.*

### 3. DBR lasers electronic control

Pigttailed DBR lasers are integrated in an electronic card, that supplies current to the three sections, and feedback control loops, with computer support.

Firstly, the laser undergoes fast characterizations (a few seconds), to define its look-up table, that is the required values of  $I_{\text{active}}$ ,  $I_{\text{phase}}$  and  $I_{\text{Bragg}}$ , to obtain the required power (typically 20mW) and ITU wavelength, with maximum SMSR.

Current sources on the electronic cards, for phase and Bragg sections, must be optimized to reduce noise. Indeed, as carriers densities are not blocked in these sections, the least noise on  $I_{\text{phase}}$  and  $I_{\text{Bragg}}$  generates index variations, thereby phase variations, and drastically degrade linewidth. The effect increases with tuning efficiency, phase length and  $L_{\text{eff}}$ . We obtain, with modules integrated in electronic card, linewidth below 10MHz over the whole tuning range.

Wavelength is measured from the rear facet with a wavelength locker (2 photodiodes and a Fabry-Perot etalon), and corrected by adjusting  $I_{\text{phase}}$ .

For power control, two solutions exist. Either front facet output power is collected with a coupler. Or rear facet (transmitted through Bragg grating) is monitored, but the ratio between front and rear power depends on the position on the mode, i.e. the difference  $\lambda_{\text{Fabry-Perot}} - \lambda_{\text{Bragg}}$ . It is then necessary to ensure concurrently mode position stabilization. In both cases, power is maintained constant by adjusting  $I_{\text{active}}$ .

But the major difficulty is mode control, that is to avoid SMSR degradation, and especially mode hops. The problem is to find a parameter, easy to measure in module, with characteristics representative of the position on the mode. Output power has often been used as monitoring [12,13], as it varies along the mode, as shown in figure 7. But for high powers, non linear effects appear, that shift power maxima to the left edge of the modes, or even suppress these maxima [14]. To limit these effects, one can weaken modes interactions with shorter active section length, leading to larger free spectral range, or increase Bragg filter selectivity with smaller  $\kappa$ .  $I_{\text{Bragg}}$  is dithered, with an extremely low frequency (a few Hz) to avoid spectral linewidth degradation, and  $I_{\text{Bragg}}$  is adjusted to maintain  $dP/dI_{\text{Bragg}}$  variation constant.

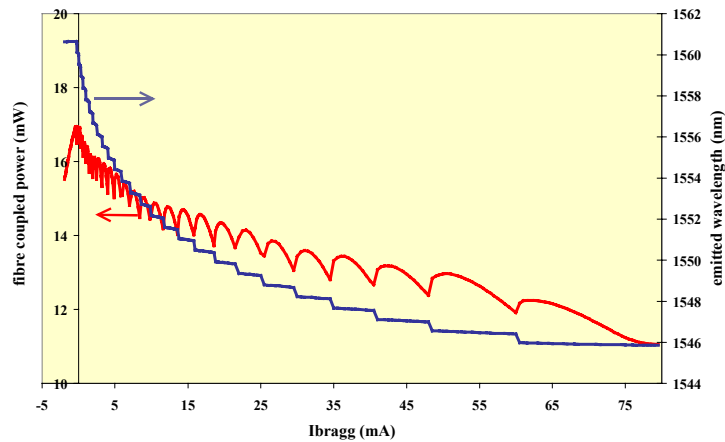


*figure 7 : wavelength and power variations with  $I_{\text{Bragg}}$ , for  $I_{\text{active}}=150\text{mA}$ .*

#### 4. DBR long-term reliability

Reliability is a key factor for DBR tunable lasers. Indeed, simultaneous power, wavelength, and mode locking can ensure stable performances with aging, in particular the absence of mode hops, when the laser remains on a ITU wavelength. But when the device is tuned to another ITU wavelength, the electronic control card applies the set of currents ( $I_{\text{active}}$ ,  $I_{\text{phase}}$  and  $I_{\text{Bragg}}$ ) determined at the device beginning of life. Hence laser degradations must remain small enough to ensure locking algorithm convergence towards the desired ITU wavelength. In particular, if the tuning characteristic  $\lambda = f(I_{\text{Bragg}})$  shifts strongly, the laser might tune to another longitudinal mode, and the wavelength locker would converge to a wrong ITU wavelength.

Bragg section aging is the main concern, as it operates with an unclamped carrier population: any aging degradation leads to a carrier density variation, hence modifying the Bragg wavelength of the mirror. Active section is expected to behave as standard Fabry-Perot lasers with the same technological process (buried ridge structure).

A study has been performed on 20 of our DBR lasers. Characteristics are first stabilized during 48 hours burning ( $100^\circ\text{C}$ ,  $I_{\text{active}}=300\text{mA}$ ,  $I_{\text{Bragg}}=300\text{mA}$ ), then monitored during 2000 hours accelerated aging ( $80^\circ\text{C}$ ,  $I_{\text{active}}=200\text{mA}$ ,  $I_{\text{Bragg}}=100\text{mA}$ ). Figure 8 shows, on a typical chip, the extremely small tuning curve shift along 2000h post-burning accelerated aging. Figure 9 demonstrates that this shift, normalized with the mode length, is below 10% on most of the 20

tested devices, and has 5% average absolute value, showing the high quality of our Q1.45 bulk material, and our current injection characteristics stability.

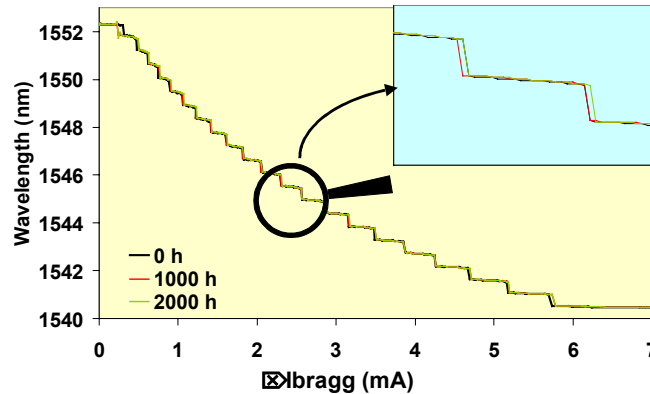


figure 8: typical tuning curve shift during 2000h post-burning accelerated aging.

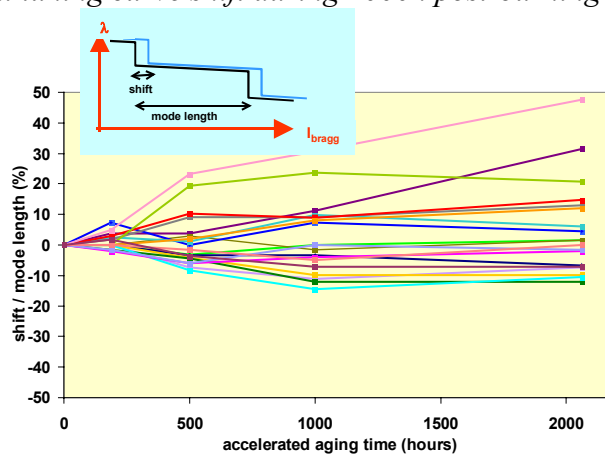


Figure 9 : 12<sup>th</sup> mode normalized shift for the 20 tested devices, during 2000h post-burning accelerated aging.

Other laboratories showed larger tuning curve shifts on their DBRs. Attributing this shift to increased non-radiative recombinations, they proposed a model that corrects the initial look-up table by extrapolating from the shift of the lasing Fabry-Perot mode [15].

## 5. New functionalities : amplifier and modulator sections

### 5.1 Semiconductor optical amplifier (SOA)

DBR lasers provide high output power, because light is emitted from the active section, and not through an absorbing and reflecting Bragg section, which enables to avoid SOA section. Still, we studied the integration of a SOA section, as it presents several advantages :

- power is provided outside cavity. Power control is totally independant from wavelength and mode control. Moreover, constraints on the active section design are loosened : active section length can be decreased, to enlarge FSR, thereby making mode control easier.
- The DBR behavior is very little affected by SOA current. In particular cavity or thermal interactions are extremely weak. The SOA section can thus be used as an optical gate, that turns off emission during  $I_{\text{active}}$  ramp, or tuning, or to allow look-up table recalibration.
- DBR lasing requires reflectivity at the active section facet. Thus if an integrated modulator is required, this modulator section cannot be added at the active section end, but compulsorily at

the Bragg section end, where emitted power is much weaker. An SOA section is then necessary to maintain power comparable with standard DFB lasers integrated with a modulator.

As the SOA section provides a high gain, and has an important reflection from the Bragg section (around  $\lambda_{\text{Bragg}}$ ), the output facet reflectivity must be extremely low to avoid SOA lasing, leading to multicavity DBR-SOA behavior, and tuning curve irregularities. The SOA section is thus tapered (ridge width reduced from 1.5 to 0.8 $\mu\text{m}$  on the last 200 $\mu\text{m}$ ), 10° tilted, and 0.01% antireflection coated.

With such a device, we obtained more than 20mW coupled output power at  $I_{\text{SOA}}=150\text{mA}$ , with unchanged tuning characteristics. And SOA as a gate seems promising, as  $\lambda_{\text{Bragg}}$  varies by less than 0.1nm for  $I_{\text{SOA}}$  ranging from 0 to 200mA, whereas it shifts by 0.5nm for the same  $I_{\text{active}}$  range.

## 5.2 Electroabsorption modulator (EAM) section

Direct modulation on a SG-DBR has been demonstrated over 40nm at 2.5Gb/s, but transmission distance is limited (75km with 4 to 6dB penalty) [16]. For most applications, a high quality modulated signal is required, which imposes the integration of an EAM section.

We use an EAM structure optimized to reduce sensitivity to  $\Delta\lambda$ , that demonstrated 2.5Gb/s transmission over 1000km standard fiber, over 20nm  $\Delta\lambda$  variations ( $\Delta\lambda = 45$  to 65nm) [17], and transmitted at 10Gb/s over 90km standard fiber. Excellent results have been demonstrated on a DBR integrated with SOA and multi-quantum well EAM, over 9nm tuning range, with 1mW average modulated power : 2.5Gb/s transmission over 681km (RF extinction ratio >14dB with  $V_{\text{EAM}}=2 V_{\text{peak to peak}}$ ), and 10Gb/s over 82km (RF extinction >8.5dB with  $V_{\text{EAM}}=1.7 V_{\text{peak to peak}}$ ) [18].

## 6. Comparison between DBR and SG-DBR

Currently, SG-DBR lasers integrated with an SOA are very promising candidates for tunable lasers applications, because they are becoming industrially reliable, and allow high power and fast tuning over more than a whole C or L band.

As a comparison, DBR lasers have slightly inferior performances in terms of tuning range (only half C or L band), and possibly in tuning speed, due to Bragg currents up to 50mA (compared to 15mA in SG-DBR) creating more thermal effects.

Still, they could be very attractive depending on the applications, as they present several important advantages :

- DBR devices are much simpler, with only 3 sections. SG-DBR requires two bragg sections, and due to the insufficient emitted power (<20mW in fiber) an SOA output section is integrated, leading to a 5-sections device. This has an impact on industrial yield, on electronic control complexity, and imposes to monitor front facet output power for power monitoring.
- Mode control, which is the major concern for these tunable devices, only demands one current ( $I_{\text{bragg}}$ ) dithering and adjustment on a DBR. Whereas for a SG-DBR, both front and rear Bragg sections currents must be dithered, at different frequencies, to monitor simultaneously parameters variations (commonly  $V_{\text{active}}$ ) relatively to front and rear Bragg currents, and adjust  $I_{\text{Bragg rear}}$  and  $I_{\text{Bragg front}}$  consequently.
- EAM characteristics (extinction, on-state absorption, chirp, ...) highly depend on the detuning  $\Delta\lambda$  between lasing wavelength and modulator absorption-edge wavelength. Good characteristics can be maintained over a 16nm DBR tuning range, but not over the whole 40nm tuning range of an SG-DBR. EAM integration has been demonstrated on a widely tunable laser (SG-DBR-SOA-EAM), providing 2.5Gb/s modulation over 40nm tuning range, with more than 10dB RF extinction ratio, provided that modulator driving voltages are adjusted according to emitted wavelength. Still, the modulated signal characteristics (chirp in particular) remain insufficient,

as transmission distance is limited to 200km [19]. To our knowledge, no 10Gb/s results have been published yet. A solution is to replace EAM by a Mach-Zehnder modulator section, that is less mature, but as well less sensitive to  $\Delta\lambda$  [20].

## Conclusion

We presented state-of-the-art of tunable laser sources, with characteristics (tuning range, tuning speed,...) addressing various transmission or routing applications. In this context, we consider DBR laser as a good compromise between simplicity (integrated device, only 3 sections, simple and mature technological process), and improved performances (16nm tuning, 13dBm coupled output power, fast tuning, ...). We took the stock on the optimizations that resulted in a device with leading performances, and on the aspects of electronic control, aging, and new functionalities integration (SOA, EAM) at the center of current studies.

- [1] D.M. Adams et al., Electronics Letters, May 2001, Vol.37, No.11, pp.691-693.
- [2] H. Hatakeyama et al., Optical Fiber Communication Conference 2002, WF2, pp.205-206.
- [3] B. Pezeshki et al., IEEE Photonics Technology Letters, Oct 2002, Vol.14, No.10, pp.1457-1459.
- [4] D. Anthon et al., Optical Fiber Communication Conference 2002, Tu07, pp.97-98.
- [5] K.J. Knopp et al., LEOS 2001, TuA1.3.
- [6] H. Debrégeas-Sillard et al., IEEE Photonics Technology Letters, Jan 2001, Vol.13, No.1, pp.4-6.
- [7] H. Debrégeas-Sillard et al., European Conference on Optical Communications 2002, P2.29.
- [8] P.J. Rigole et al., Electronics Letters, Dec 1996, Vol.32, No.25, pp.2352-2354.
- [9] [www.agilitycom.com](http://www.agilitycom.com)
- [10] T. Liljeberg et al., Semiconductor Laser Conference 2002, TuB1, pp.45-46.
- [11] D.C.F. Reid et al., Optical Fiber Conference 2002, ThV5, pp.541-543.
- [12] J.E. Johnson et al., IEEE Journal of Selected Topics in Quantum Electronics, March/April 2001, Vol.7, No.2, pp168-177.
- [13] H. Ishii et al., Journal of Lightwave Technology, March 1998, Vol.16, No.3, pp.433-441.
- [14] A.P. Bogatov et al., IEEE Journal of Quantum Electronics, July 1975, Vol. 11, No.7, pp.510-515.
- [15] D.A. Ackerman et al., IEEE Journal of Quantum Electronics, Nov. 2001, Vol.37, No.11, pp.1382-1387.
- [16] M.L. Majewski et al., Optical Fiber Communication Conference 2002, ThV2, pp.537-538.
- [17] H. Debrégeas-Sillard et al., IEEE Photonics Technology Letters, Nov. 1999, Vol.11, No.11, pp.1485-1487.
- [18] J.E. Johnson et al., LEOS 2001, TuA2.3, pp.37-38.
- [19] Y.A. Akulova et al., Optical Fiber Communication Conference 2002, ThV1, pp.536-537.
- [20] E.J. Skogen et al., Semiconductor Laser Conference 2002, TuB3, pp.49-50